
NONPARAMETRIC FUNCTIONAL CALIBRATION OF COMPUTER MODELS

D. Andrew Brown and Sez Atamturktur

Clemson University

Supplementary Material

Here the reader may find additional material, including the full conditional distributions for implementing the proposed model and supplementary figures.

S1 Full Conditional Distributions for the Proposed Model

Under the reparameterized version of Model (2.4) we have the following full conditional distributions needed for a Gibbs sampling algorithm:

$$\begin{aligned}
 \pi(\boldsymbol{\theta}_1^{(x)} | \xi, \nu, \lambda_\theta, \lambda_y, \mathbf{y}) &\propto \exp \left\{ -\frac{\lambda_y}{2} (\mathbf{y} - \boldsymbol{\eta}(\boldsymbol{\theta}_1^{(x)}, \exp\{-e^\xi\}))^T (\mathbf{y} - \boldsymbol{\eta}(\boldsymbol{\theta}_1^{(x)}, \exp\{-e^\xi\})) \right\} \\
 &\quad \times \exp \left\{ -\frac{\lambda_\theta}{2} (\mathbf{g}(\boldsymbol{\theta}_1^{(x)}) - \mu_\theta \mathbf{1})^T \mathbf{R}_\nu^{-1} (\mathbf{g}(\boldsymbol{\theta}_1^{(x)}) - \mu_\theta \mathbf{1}) \right\} \\
 \pi(\xi | \boldsymbol{\theta}_1^{(x)}, \lambda_y, \mathbf{y}) &\propto \exp \left\{ -\frac{\lambda_y}{2} (\mathbf{y} - \boldsymbol{\eta}(\boldsymbol{\theta}_1^{(x)}, \exp\{-e^\xi\}))^T (\mathbf{y} - \boldsymbol{\eta}(\boldsymbol{\theta}_1^{(x)}, \exp\{-e^\xi\})) + \xi - e^\xi \right\} \\
 \lambda_y | \boldsymbol{\theta}_1^{(x)}, \xi, \mathbf{y} &\sim \text{Ga} \left(a_y + \frac{N}{2}, b_y + \frac{1}{2} (\mathbf{y} - \boldsymbol{\eta}(\boldsymbol{\theta}_1^{(x)}, \exp\{-e^\xi\}))^T (\mathbf{y} - \boldsymbol{\eta}(\boldsymbol{\theta}_1^{(x)}, \exp\{-e^\xi\})) \right) \\
 \lambda_\theta | \boldsymbol{\theta}_1^{(x)}, \nu &\sim \text{Ga} \left(a_\theta + \frac{N}{2}, b_\theta + \frac{1}{2} (\mathbf{g}(\boldsymbol{\theta}_1^{(x)}) - \mu_\theta \mathbf{1})^T \mathbf{R}_\nu^{-1} (\mathbf{g}(\boldsymbol{\theta}_1^{(x)}) - \mu_\theta \mathbf{1}) \right) \\
 \pi(\nu | \boldsymbol{\theta}_1^{(x)}, \lambda_\theta) &\propto |\mathbf{R}_\nu|^{-1/2} \exp \left\{ -\frac{\lambda_\theta}{2} (\mathbf{g}(\boldsymbol{\theta}_1^{(x)}) - \mu_\theta \mathbf{1})^T \mathbf{R}_\nu^{-1} (\mathbf{g}(\boldsymbol{\theta}_1^{(x)}) - \mu_\theta \mathbf{1}) + \nu - e^\nu \right\} \\
 &\quad \times (1 - \exp\{-e^\nu\})^{b_\theta - 1}.
 \end{aligned} \tag{S1.1}$$

S2 Supplementary Tables and Figures

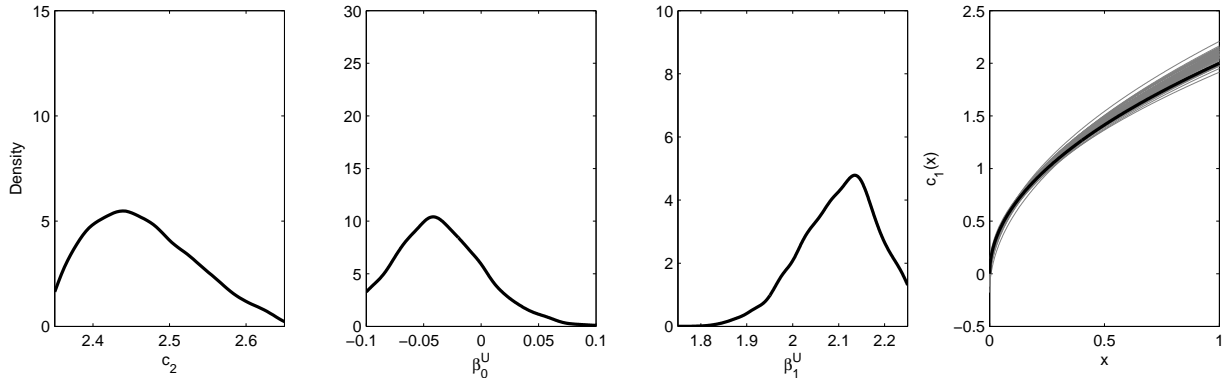


Figure 1: Smoothed approximate posterior distributions of c_2 , β_0^U , and β_1^U (first three panels from the left) when replacing the GP prior with $\theta_1(x) = \beta_0 + \beta_1\sqrt{x}$. The far right panel plots realizations of the estimating curves (grey lines) based on draws of β_0^U and β_1^U from their posterior, along with the true function for reference (heavy black line).

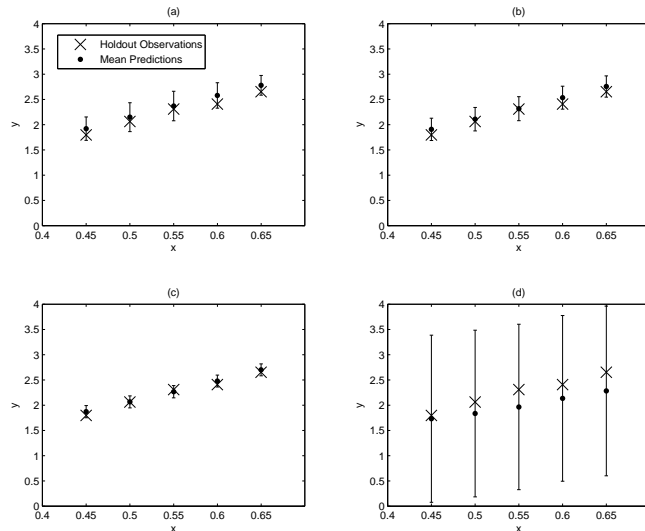


Figure 2: Posterior predictions at holdout settings with approximate 95% error bars under (a) $\theta_1(x)$ constrained at x_1 and x_N , (b) θ_2 constrained between tight prior bounds, (c) $\theta_1(x) = \beta_0 + \beta_1\sqrt{x}$, and (d) θ_1 assumed constant.

Link	Logit	Probit	Cumulative Log-Log	Identity
RMSPE	0.0902	0.0995	0.0957	0.0757

Table 1: Root mean squared predictive error (RMSPE) at the holdout settings for each link function.

S2. SUPPLEMENTARY TABLES AND FIGURES3

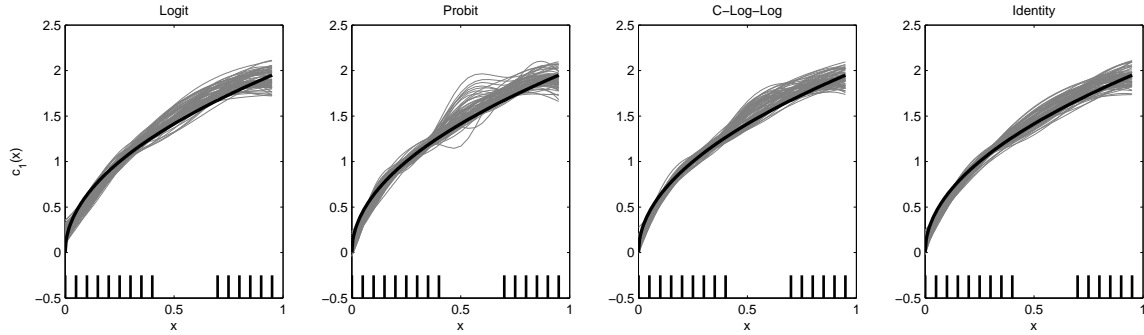


Figure 3: Posterior sample paths of $c_1(\cdot)$ obtained from using the logit, probit, c-log-log, and identity link functions with the simulated data example. The tick marks at the bottom indicate the settings for the training data.

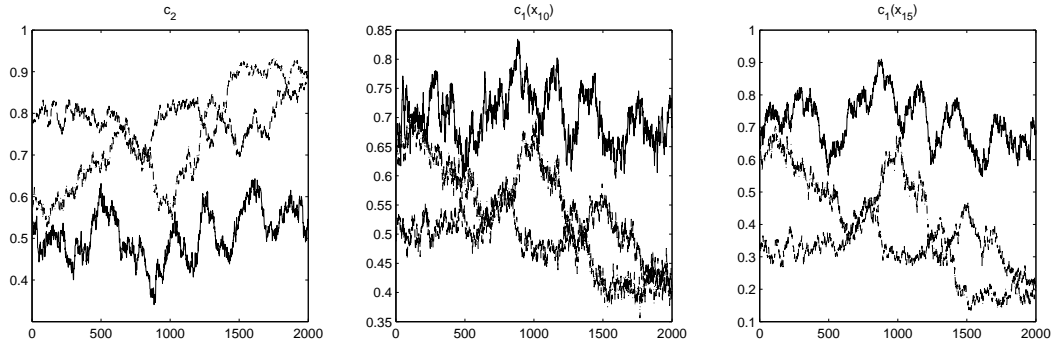


Figure 4: Trace plots of sampled values of the calibration parameters c_2 , $c_1(x_{10})$, and $c_1(x_{15})$ for three different chains (with different initial values) under vague priors for both $c_1(\cdot)$ and c_2 .

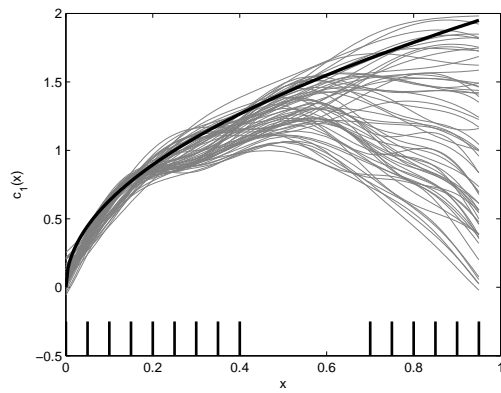


Figure 5: Sample paths of $c_1(\cdot)$ obtained from combining the three chains in Figure 4. The tick marks at the bottom indicate the settings for the training data.

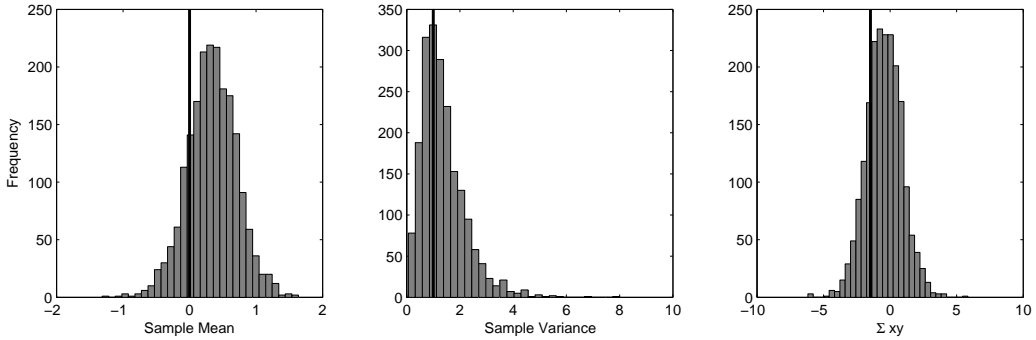


Figure 6: Histograms of sample statistics calculated from 2,000 replicated datasets from the posterior predictive distribution: T_1 = sample mean (left panel), T_2 = sample variance (middle panel), $T_3 = \sum_{i=1}^N x_i y_i$ (right panel). The dark vertical lines are at the observed statistics from the field data.

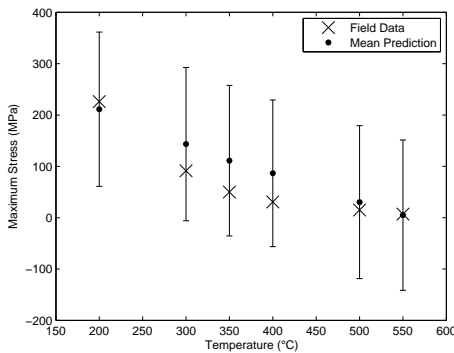


Figure 7: Posterior predictions of maximum stress from the glide VPSC model with approximate 95% error bounds at the observed experimental settings.